Removal of COD, TOC, and color from pulp and paper industry wastewater through electrocoagulation

Ravi Shankar, Lovjeet Singh, Prasenjit Mondal*, Shri Chand

Department of Chemical Engineering, Indian Institute of Technology Roorkee, Roorkee 247667, Uttarakhand, India
Tel. +91 1332 285181; Fax: +91 1332 276535; email: mondal2001@gmail.com

ABSTRACT

The present paper deals with the treatment of paper and pulp industry wastewater through electrocoagulation in a batch reactor using aluminum as a sacrificial electrode. The effect of various parameters such as pH, treatment time, current density, and inter-electrode distance on the removal of chemical oxygen demand (COD), total organic carbon (TOC), and color from pulp and paper industry wastewater has been investigated to determine the optimum process conditions. A central composite design has been used to design the experimental conditions for developing mathematical models to correlate the removal efficiency with the process variables. The optimum process condition for the maximum removal of COD, TOC, and color from pulp and paper industry wastewater have been found to be as pH: 7, treatment time: 75 min, current density: 115 A/m^2, and inter-electrode distance: 1.5 cm with a combined desirability index value of 0.816. Under optimum operating conditions, the percent removals of COD, TOC, and color are ≈77, 78.8, and 99.6%, respectively. The proposed models are found suitable to predict the percent removals of COD, TOC, and color with the error limits of ±7, ± 9, and + 2 to −6%, respectively. The sludge and scum produced during the process have been characterized to assess their potential as a source of energy and aluminum recovery.

Keywords: Wastewater; Electro-coagulation; COD; TOC; Colour; Electrode; Pulp and paper industry

1. Introduction

Wastewater from pulp and paper industry contains chlorinated compounds (measured as AOX), fatty acid, tannins, resin acid, phenols and its derivatives, lignin and its derivatives, sulfur and sulfur compounds [1,2]. All of these compounds are responsible for high total organic carbon (TOC), chemical oxygen demand (COD), color, AOX, and low biodegradability index (<0.4) [3]. These compounds create a condition that is toxic to aquatic life and exhibit strong mutagenic effects. So, the removal of these pollutants from effluent becomes necessary before its discharge to main water sources.

Various conventional techniques available for the treatment of pulp and paper industry wastewater such as adsorption [4,5], chemical oxidation [6,7], and chemical coagulation [8,9] require chemicals and produce secondary pollutants. Further, the biological processes are normally not effective for the treatment of pulp and paper industry wastewater due to its low

*Corresponding author.

biodegradability index (<0.4). Under this backdrop, electrocoagulation (EC) technique is getting strong research interest around the world for the treatment of pulp and paper industry wastewater because it produces coagulants *in situ* by dissolving electrodes in the cell which helps in the removal of the pollutants producing negligible secondary pollutants [10]. The major phenomena taking place during the EC process are anode oxidation, reduction of water at cathode, electrolytic reaction in electrode surface, and adsorption of colloidal pollutants on coagulant followed by removal through sedimentation or flotation. Some important reactions are shown through Eqs. (1–4).

$$\text{Oxidation of anode: } M^{(s)} \rightarrow M^{n+}(aq) + ne^- \tag{1}$$
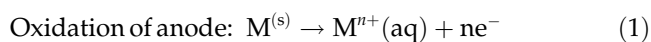
Reduction of water at cathode:
$$nH_2O + ne^- \rightarrow n/2H_2 + nOH^- \tag{2}$$
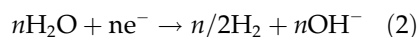
Reaction at alkaline conditions:
$$M^{n+} + nOH^- \rightarrow M(OH)_n \tag{3}$$
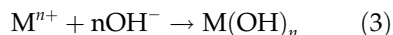
Reaction at acidic conditions:
$$M^{n+} + nH_2O \rightarrow M(OH)_n + nH^+ \tag{4}$$

The treatment of real pulp and paper industry wastewater using EC process have been reported by some investigators, [11–14] dealing with the removal of color, COD, and biological oxygen demand. However, hardly any literature is available, which deals with the removal of TOC and modeling for finding the correlation among various operating parameters and the removal efficiencies (percent removals) of COD, TOC, and color. The studies on sludge characterization and its management are also less reported.

In the present paper, the removal of COD, TOC, and color from real pulp and paper industry wastewater through EC in a batch reactor has been presented. The effect of parameters such as current density, pH, treatment time, and inter-electrode distance on the removal efficiencies has been investigated to determine the optimum process conditions. A central composite design (CCD) has been used to design the experimental conditions for developing mathematical models to correlate the removal efficiencies with the process variables and study the interactive influences of parameters on the removal efficiencies of COD, TOC, and color. The sludge and scum generated during the process have been characterized to assess their potential to be used as energy source and aluminum recovery.

2. Experimental methods

2.1. Materials

The wastewater treated in the present study was black liquor obtained from an agro-based Indian paper mill. It was a medium-scale industry having paper production capacity ~14,500 TPA and using bagasse as the raw material. The wastewater was stored at 4°C to conserve its characteristics. The initial characteristics (after dilution) of the real pulp and paper industry wastewater used for experimental study are shown in Table 1. The aluminum electrode was sourced from a local market in Roorkee. All the chemicals used in the present study were of A. R. grade and purchased from M/s Himedia Ltd., Mumbai.

2.2. Experimental setup

For EC studies, the batch reactor of volume 1.52 liters, made of Perspex glass, was used. Aluminum metal plates with an area of $8 \times 8\,cm^2$ acted as electrodes. The electrodes were positioned vertically and parallel to each other with an inner gap of 1–3 cm. These were kept at 5 cm above the bottom surface of reactor for the proper mixing by the magnetic stirrer. The active area of each electrode used for EC was $64\,cm^2$. The electrodes were connected through a parallel arrangement. DC supply (0–30 V, 0–5 A) was given to the electrodes in monopolar mode according to the required current intensity and each experiment was carried out at constant current condition. The schematic diagram of the experimental setup is shown in Fig. 1.

2.3. Experimental procedure

2.3.1. Pretreatment and characterization of electrodes

The electrode plates were cleaned manually by abrasion with sandpaper followed by further cleaning with 15% HCl for cleaning and washing with distilled

Table 1
Initial characteristics of wastewater used for experimental studies

Parameters	Values
COD (mg/l)	7,000
Color (Hazen)	10,312
pH	11.68
TOC (mg/l)	2,825
TC (mg/l)	2,878
IOC (mg/l)	53

Note: TC: Total carbon, IOC: Inorganic carbon.
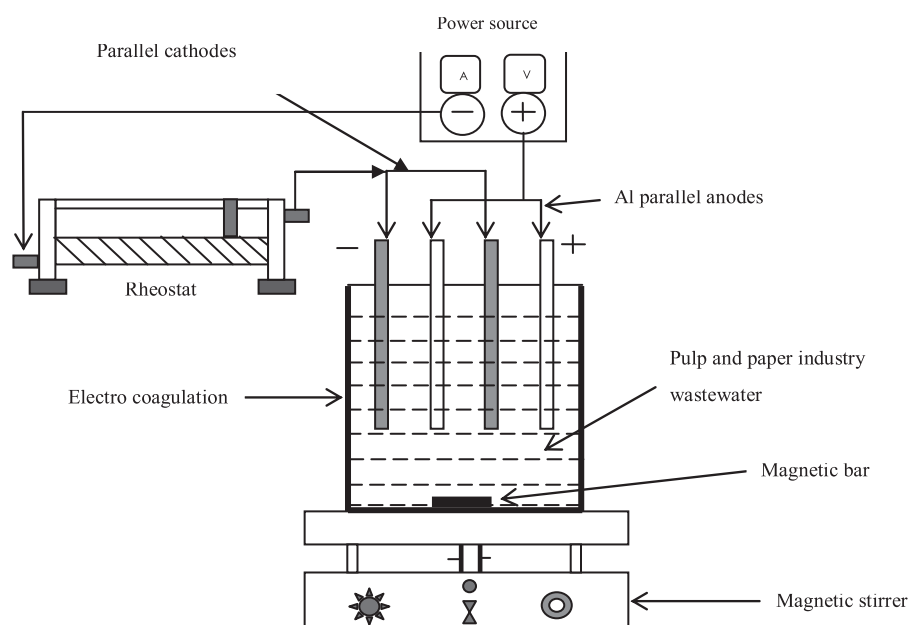
Fig. 1. Schematic diagram of the experimental setup.

water prior to its use. The electrodes were dried for half an hour in an oven and weighted.

2.3.2. Batch EC studies

Each 1.5 L of industrial solution was taken in the reactor and a desired amount of NaCl 1 mg/l was added. Then, the pH of the solution was adjusted using 0.1 M HCl and 0.1 M NaOH solutions. The distance between electrodes was set at desired value (1–3 cm). The magnetic stirrer and DC power supply were kept at desired value. The experimental conditions (current density, pH, distance between electrodes, and treatment time) were decided on the basis of CCD of experiments as shown in Table 2. A total of 25 experiments were performed to obtain the removal of COD, TOC, and color at different process conditions. After the completion of experiment, the sample was centrifuged for 30 min at 10,000 RPM and the final COD, TOC, and color of the clear solution were measured.

Finally, COD, TOC, and color removals (obtained through experiments) were used to develop the empirical correlation using design expert software and the optimum process conditions were determined on the basis of desirability index.

2.3.3. Analytical procedures

COD of samples was measured according to closed reflux colorimetric method using COD analyzer

(SN 09/17443 Lovibond Spectrophotometer) after adding the desired chemicals and providing digestion period of 2 h in COD reactor (ET 125 SC Lovibond) [15]. TOC was measured by TOC analyzer (TOC-Vcph Shimadzu) as per high temperature catalytic combustion method by combustion of organic compounds at 680°C [15]. The clear sample was analyzed by UV-Spectrophotometric method for color units according to Canadian Pulp and Paper Association (CPPA) standard method [16]. Before measurement, the pH of sample was adjusted to 7.6 using 0.1 M H_2SO_4 or 0.1 M NaOH. The absorbance values were transformed into color units (CU) according to the equation [16]:

$$CU = 500 \times \frac{A_2}{A_1} \qquad (5)$$

where A_1 is the absorbance of 500 CU platinum–cobalt standard solution ($A_{465} = 0.132$) and A_2 is the absorbance of the effluent sample.

The experimental data were used to find out the optimum process conditions as well as to regress mathematical expressions correlating percent removals of COD, TOC, and color with the process parameters through ANOVA using design expert software. Errors on COD, color, and TOC removal were computed as per Eq. (6).

$$\% \text{ Error} = \frac{(\text{Experimental value} - \text{Modeled value})}{\text{Modeled value}} \times 100 \qquad (6)$$

Table 2
Four-factor five-level central composite design for deciding experimental conditions

Experiment no.	A: Current density (A/m^2)	B: pH	C: Distance between electrodes (mg/l)	D: Time (min)
1	−1	−1	−1	−1
2	1	−1	−1	−1
3	−1	1	−1	−1
4	1	1	−1	−1
5	−1	−1	1	−1
6	1	−1	1	−1
7	−1	1	1	−1
8	1	1	1	−1
9	−1	−1	−1	1
10	1	−1	−1	1
11	−1	1	−1	1
12	1	1	−1	1
13	−1	−1	1	1
14	1	−1	1	1
15	−1	1	1	1
16	1	1	1	1
17	−2	0	0	0
18	2	0	0	0
19	0	−2	0	0
20	0	2	0	0
21	0	0	−2	0
22	0	0	2	0
23	0	0	0	−2
24	0	0	0	2
25	0	0	0	0

Note: The five levels of current density (A) are: $2 = 180\,A/m^2$, $1 = 145\,A/m^2$, $0 = 110\,A/m^2$, $−1 = 75\,A/m^2$, $−2 = 40\,A/m^2$; for pH (B): $2 = 9$, $1 = 8$, $0 = 7$, $−1 = 6$, $−2 = 5$; for distance between electrode (C): $2 = 3.00$, $1 = 2.5$, $0 = 2$, $−1 = 1.5$, $−2 = 1.0$; and for treatment time (D): $2 = 90\,min$, $1 = 75\,min$, $0 = 60\,min$, $−1 = 45\,min$, $−2 = 30\,min$.

2.3.4. Characterization of sludge

The sludge and scum generated during the EC process were characterized by using SEM-EDAX model Quanta 200 F, FTIR Model Nicolet 6700, and TGA/DTA/DTG model EXSTAR TG/DTA 6300. The thermal analysis was carried out under oxidizing atmosphere of air under flow rate of 200 ml/min. The range of temperature was 25–1,000℃. The details of temperature profile for TGA analysis of scum and sludge are given in Table 3.

3. Results and discussion

The effect of various process parameters on the removal efficiencies, development of models and their

Table 3
Temperature profiles for TGA analysis of scum and sludge

Sample	Heating rate (℃/min)	Transition zone	Temperature range (℃)
Scum	10	1st zone	25–200
		2nd zone	200–500
		3rd zone	500–1,000
Sludge	10	1st zone	25–200
		2nd zone	200–500
		3rd zone	500–1,000

validation, and characterization of sludge and scum to assess its suitability for energy production is described below.

3.1. Effects of process parameters

The effects of initial pH and current density on the removal of COD, TOC, and color are shown in Fig. 2. From Fig. 2(a)–(c), it is evident that the maximum removal efficiencies for the removal of COD, TOC, and color are achieved at the pH value of around 7. During electrocoagulation, the generated metallic cations interact with OH^- to form hydroxides, which adsorb pollutants (bridge coagulation). In some cases, the hydroxides form larger lattice-like structures and sweep through the water (sweep coagulation). The cations or hydroxyl ions can also form a precipitate with the pollutants through neutralizing the charge of the colloidal particles. Further, the adhesion of bubbles to the flocs resulting electroflotation can also help in the removal of pollutants [17]. The charge and stability of the aluminum hydroxides vary significantly with pH of the solution. Since the pHzpc of aluminum varies within 7–8.3 [18], below this pH range the aluminum hydroxides are predominantly positively charged, above this pH range these become predominantly negatively charged, and in this pH range these are predominantly neutral. At the pH value of around 7, polymeric species like $Al_6(OH)_{15}^{3+}$, $Al_7(OH)_{17}^{4+}$, $Al_8(OH)_{20}^{4+}$, etc. are formed that are finally converted into $Al(OH)_3$ [19]. Freshly formed amorphous $Al(OH)_3$ has the minimum solubility and is finally polymerized into $Al_n(OH)_{3n}$, which results into dense flocs formation. The dense flocs have a large surface area which provides quick adsorption of soluble organic compounds and entrapment of colloidal particles and thus result in the maximum reduction of COD, TOC, and color by flotation and sedimentation [17]. Further at pH > 7, the predominant form of aluminum hydroxide is $Al(OH)_4^-$, which is
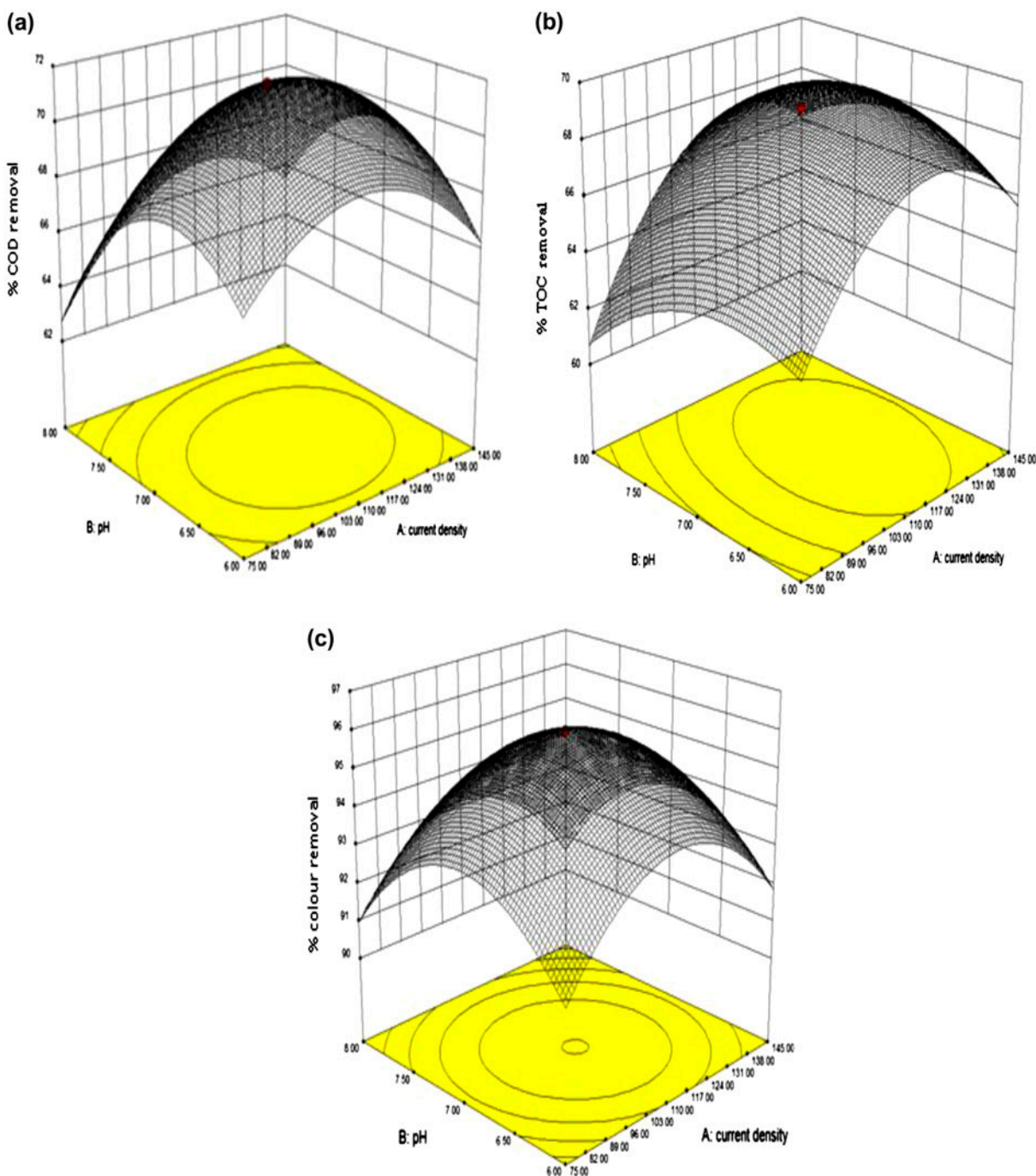
Fig. 2. Effects of intial pH and current density on removal of COD, TOC, and color (a) COD removal (b) TOC removal (c) Color removal (inter-electrode distance: 2 cm, time: 60 min).

negatively charged and thus gives lower adsorption of negatively charged pollutants resulting in lower removal of COD, TOC, and color.

At lower pH (<7), the predominating forms of aluminum hydroxide are Al^{3+}, $Al(OH)^{2+}$, and $Al(OH)_2^+$,

which favor coagulation and precipitation through neutralization of the charge on anionic colloidal particles present in the wastewater [20]. Less number of larger flocs may be responsible for the lesser removals than that achieved at pH 7.

From Fig. 2(a)–(c), it is evident that percent removal of COD, TOC, and color increases initially with the increase in current density, reaches the maximum value at around 115 A/m², and thereafter decreases. The amount of metal ion (aluminum) released into solution by electrolytic oxidation of anode material is a function of current and time and can be calculated by the Faraday's law [21]:

$$W = \frac{itM}{ZF} \tag{7}$$

where W is the metal dissolved (g), i is the current (A), t is the contact time (s), M is the molecular weight of aluminum, Z is the number of electron involved in the redox reaction ($Z = 3$), and F is the Faraday constant (96,500 C/mol).
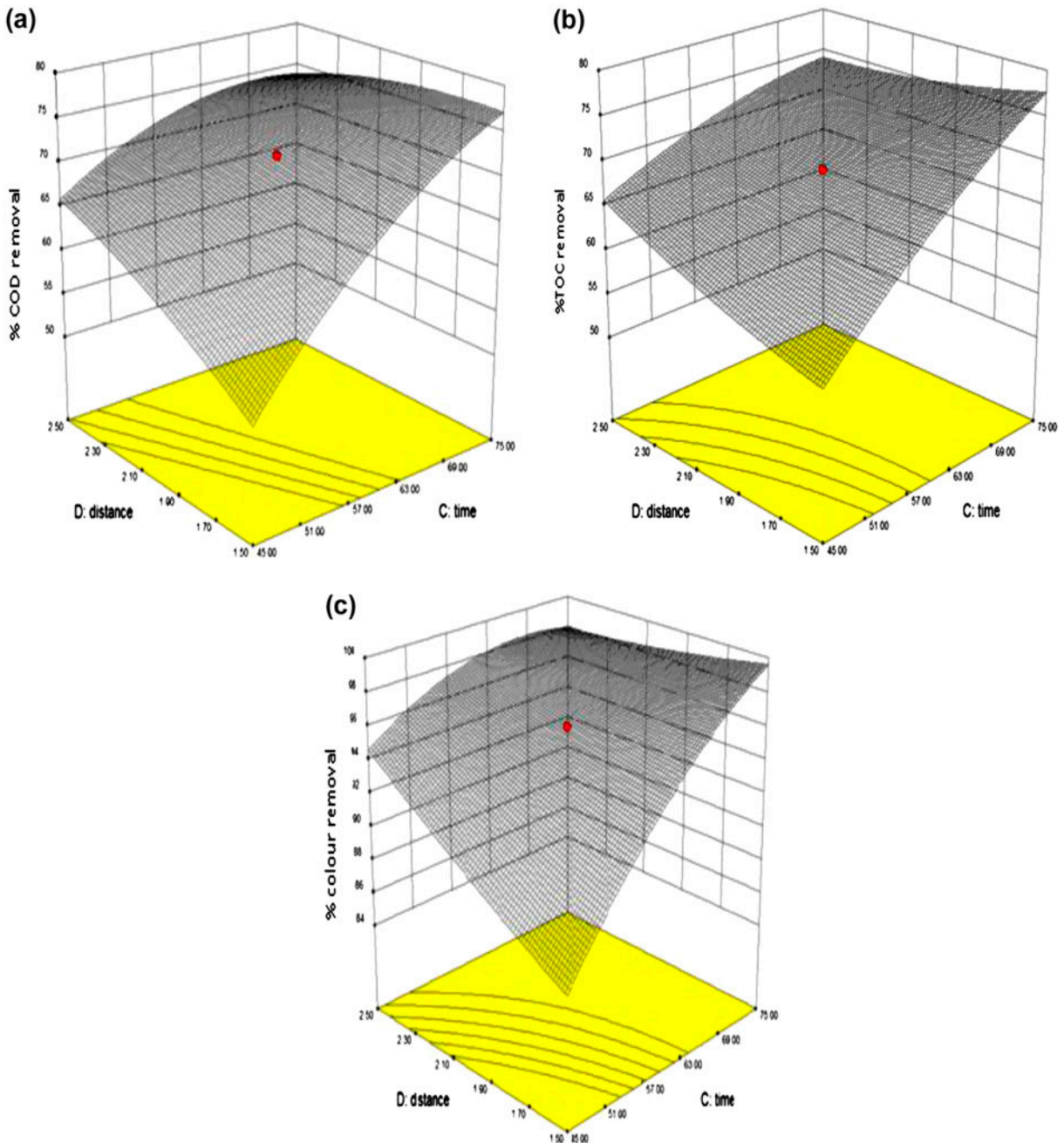
Fig. 3. Effects of inter-electrode distance and time on removal of COD, TOC, and color (a) COD removal (b) TOC removal (c) Color removal (current density: 110 A/m², pH: 7).

The initial increase in current density increases aluminum dissolution (aluminum hydroxide formation) in the solution and increases the removal efficiency via coprecipitation and sweep coagulation. In addition, the increase in current intensity also increases the gas evolution rate and decreases the size of emanating bubbles with increasing bubble density which may favor quick flotation of the particles resulting in increase in the pollutant removal efficiency [22]. However, it is observed that at higher current intensity($>120 \, A/m^2$), the removal efficiency decreases. It might be due to the increase in solution pH and its temperature, which increases the solubility of precipitates and thus reduces the removal efficiency [23]. Further, at higher current density ($>120 \, A/m^2$), the cathode passivation may occur considerably because of the monopolar electrodes in EC reactor

under DC conditions, which may also be responsible for the reduction in removal efficiency. It is also interesting to note that under the operating conditions, with the initial COD value of 7,000 mg/l, the maximum removal of COD and TOC is around 77–78%, whereas the color removal is > 99%. This indicates that the organic compounds present in the wastewater are not equally removable by electrocoagulation and the compouds responsible for color development are almost completely removable through electrocoagulation.

The effects of electrode distance and time on the removal efficiencies of COD, TOC, and color are shown in Fig. 3. From Fig. 3(a)–(c), it is noteworthy that with increase in treatment time, the COD, TOC, and color removal increases. The increase in removal with time can be explained on the basis of Faraday's
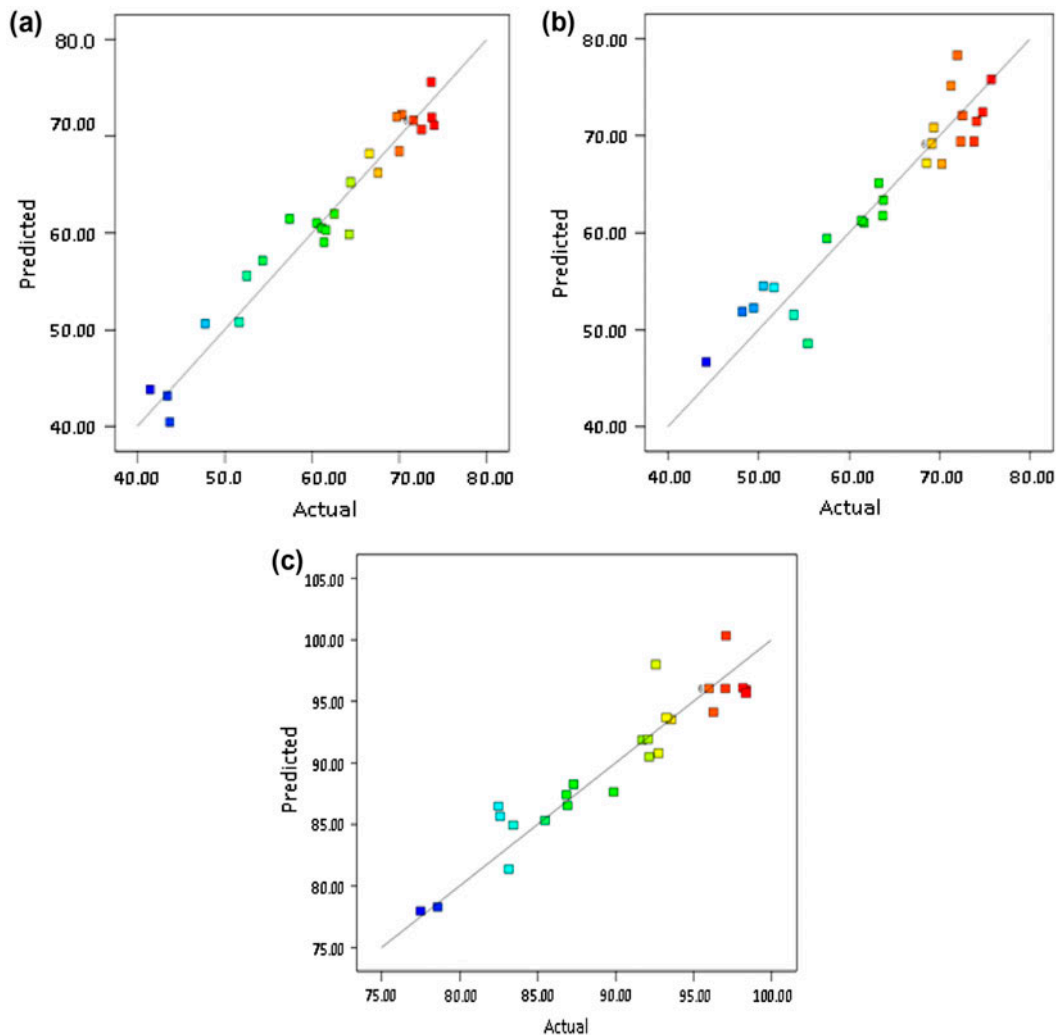
Fig. 4. Experimental and predicted percent removals of COD, TOC, and color (a) COD removal (b) TOC removal (c) Color removal.
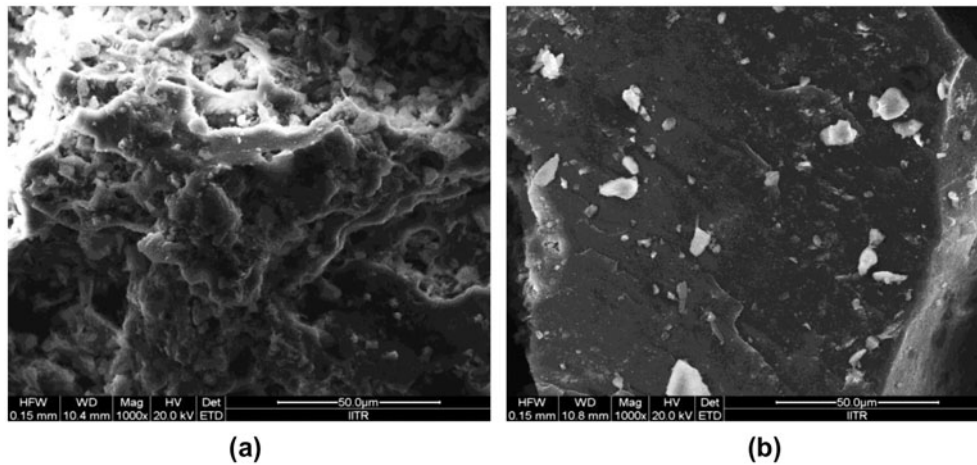
Fig. 5. SEM micrograph of scum and sludge (1,000 times magnification) (a) scum and (b) sludge.

law as expressed in Eq. (7), which shows that the rate of formation of Al ions and their flocs are proportional to treatment time. These flocs are responsible for the removal of pollutant by coprecipitation and sweep coagulation [14]. It is observed that the percent removals of COD, TOC, and color increase very fast with increase in time up to 65 min. Thereafter, the pollutant removal rates become slow and approach a steady state. The optimum time for the maximum removal was observed as 75 min.

Fig. 3(a)–(c) also shows the effects of inter-electrode distance on the percent removals of COD, TOC, and color during EC process. It has been observed that with the increase in inter-electrode distance from 1 to 3 cm, the percent removals of COD, TOC, and color increase from 56 to 65, 59 to 65, and 88 to 94%, respectively. When the inter-electrode distance is low (1 cm gap), the interaction of colloidal particles/flocs may significantly affect their settling and flotation characteristics, which results in high resistance among the particles/flocs, resulting in less removal [24].With the increase in inter-electrode distance, the hindrance

effects may reduce gradually and as a result the percent removals increase to some extent. The optimum conditions as determined on the basis of maximum desirability index value (0.816) using design expert software are: current density: 115 A/m^2, pH: 7, inter-electrode distance: 1.5 cm and treatment time: 75 min.

3.2. Model development

The proposed empirical model equations derived by using design expert software to correlate the percent removals of COD, TOC, and color with process parameters (confidence level > 95%) in actual factors are shown through Eqs. (8)–(10), respectively. Empirical models are developed because of the apparently complex nature of the EC process. where A = current density (A/m^2), B = pH, C = distance between electrode (cm), and D = time(min)

The experimental and predicted percent removals of COD, TOC, and color are shown in Fig. 4(a)–(c), respectively. It seems that the above models are suitable to predict the percent removals of COD, TOC,

$$
\begin{aligned}
\% \text{ removal of COD} = {} & 0.4009\,A + 31.9421B + 35.5739C + 2.5809D + 0.0229AB - 0.0002AD - 0.0096AC \\
& + 0.1020BD + 3.1462BC - 0.5474DC - 0.0023A^2 - 3.4320B^2 - 4.6730C^2 - 0.0136D^2 \\
& - 193.2841
\end{aligned}
$$

$$(R^2 = 0.96, F \text{ value } 24.40, P \text{ value} < 0.0001)$$

(8)

$$
\begin{aligned}
\% \text{ removal of color} = {} & 0.4638A + 21.0313B + 9.0408C + 0.7020D - 0.0049AB + 0.0001AD - 0.0045AC \\
& + 0.1528BD + 1.5325BC - 0.3308DC - 0.0019A^2 - 2.3692B^2 + 0.9733C^2 - 0.0070D^2 \\
& - 43.2709
\end{aligned}
$$

$$(R^2 = 0.90, F \text{ value } 9.98, P \text{ value} < 0.0001)$$

(9)

% removal of TOC =

$$= 0.5230A + 15.9636B + 18.1060C + 1.4578D + 0.0222AB - 0.0009AD + 0.0230AC$$
$$+ 0.1077BD - 0.6438BC - 0.4276DC - 0.0028A^2 - 1.7226B^2 + 3.1046C^2 - 0.0064D^2 \qquad (10)$$
$$- 96.2586$$

$(R^2 = 0.91, F \text{ value } 10.24, P \text{ value} < 0.0001)$

and color with the error limits of ± 7, ± 9, and $+2$ to -6%, respectively.

3.3. Scum and sludge management

Scum and sludge produced during the EC process were characterized to find out suitable option(s) for their utilization. The scanning electron micrographs (SEM) of the scum and sludge, as shown in Fig. 5(a) and (b), were developed to study the differences in their morphology. Comparing Fig. 5(a) and (b), it seems that the scum particles are more irregular and porous than the sludge particles, which may be due the floatation of these particles as scum during EC. The dense structure of sludge favors its settling.

From Fig. 6(a) and (b), it is evident that there is hardly any difference in the patterns of FTIR spectra of the scum and sludge, which supports the presence of similar types of functional groups in both scum and sludge. Broad bands in between 3,500 and 3,000 cm^{-1} are due to the O–H functional groups. Peaks at 2,925.43 and 2,851.76 cm^{-1} for scum, and 2,929.4 cm^{-1} for sludge are caused due to the presence of symmetric or asymmetric CH stretching of aliphatic acid [25]. Peaks between 1,800 and 1,300 cm^{-1} are caused due to the presence of C=C in aromatic ring and C=H stretching [26]. This range also shows the C=O. The peaks at 1,110.23 cm^{-1} for scum and 1,074.05 cm^{-1} for sludge are probably due to C–O stretching. Peaks in the wave number range of 1,000–500 cm^{-1} indicate the presence of C–H (aromatics) with strong appearance and miscellaneous oxides including silicon oxides [27]. Small and sharp peaks observed at 468.52 cm^{-1} for scum and 477.67 cm^{-1} for sludge are probably due to the C–X stretching [28]. The presence of C, O, and Si in scum and sludge as shown in their EDAX analysis in Table 4 also supports the presence of above functional groups.
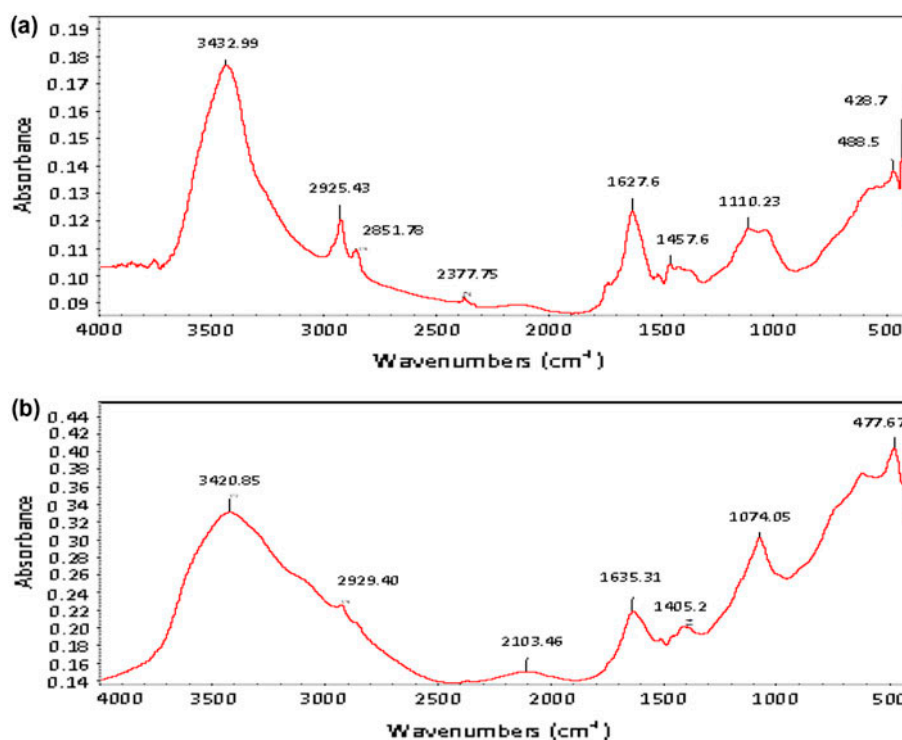
Fig. 6. FTIR spectra of scum and sludge, (a) scum and (b) sludge.

Table 4
EDAX analysis of scum and sludge

Element	Scum (wt%)	Sludge (wt%)
C	38.32	23.81
O	28.02	30.33
Na	04.55	02.92
Al	22.45	38.34
Si	01.75	01.24
S	01.94	01.55
Cl	02.98	01.81

The EDAX analysis of scum and sludge as shown in Table 4 also indicates that the aluminum content in sludge (38.3%) is more than that in scum (22.5%) and the carbon content in scum (38.3%) is more than that in sludge (23.8%). It seems that the scum can be used as a source of energy through incineration and both scum and sludge can be used to recover aluminum [29].

The thermal stabilities of scum and sludge are directly dependent on the decomposition temperature of their various functional groups and oxides. The TGA, differential thermal analysis (DTA), and differential thermal gravimetric (DTG) of scum and sludge are shown in Fig. 7(a) and (b).

The TGA shows the loss in weight due to moisture and some low molecular weight compounds from 25 to 200°C. The rate of weight loss increases between 200 and 500°C due to evolution of CO_2 and CO for both
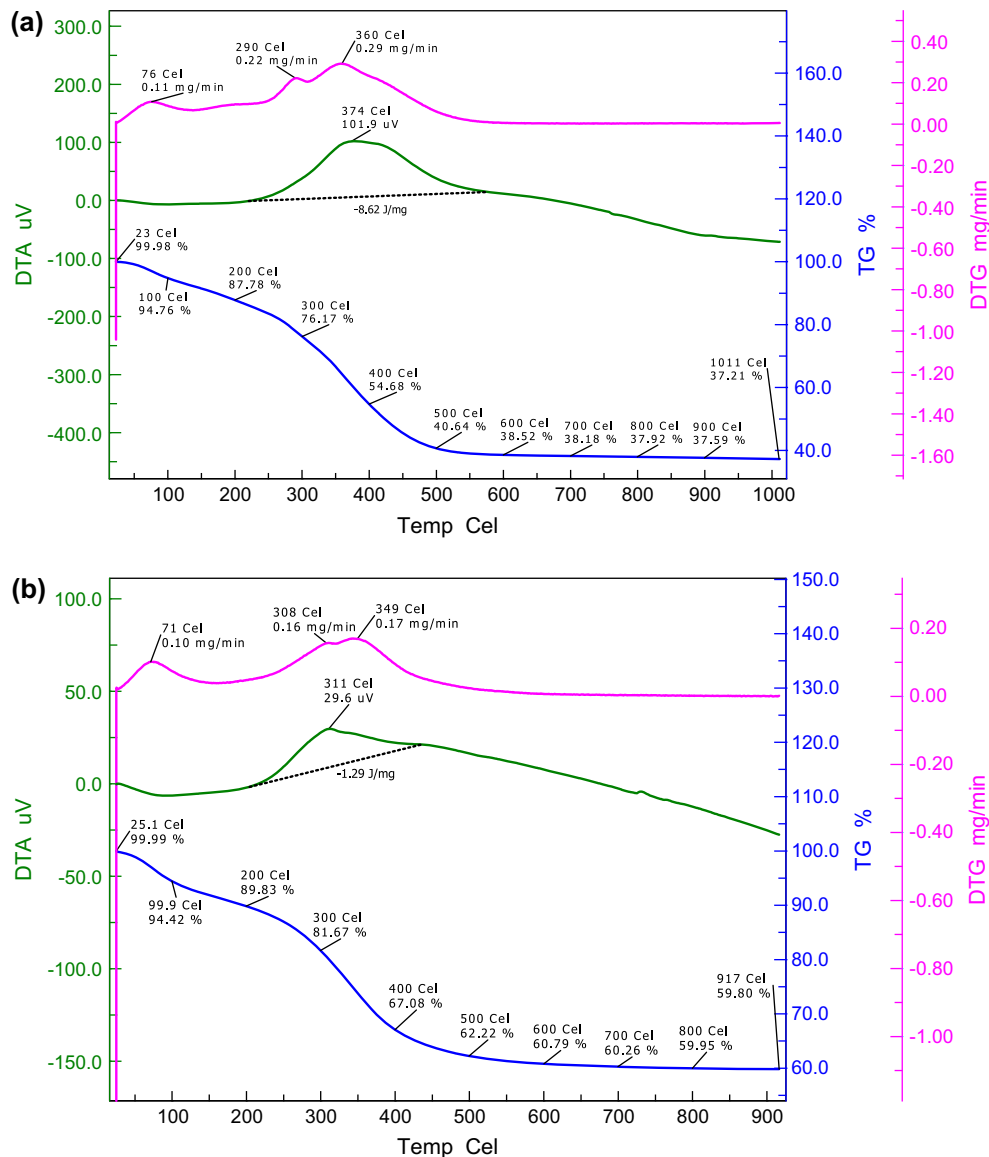
Fig. 7. Thermo gravimetric analysis of scum and sludge (a) scum (b) sludge.

scum and sludge. The weight loss of scum is found to be more as compared to sludge, which is due to the less carbon content in sludge with respect to scum as evident from Table 4. The weight loss due to the heating in the temperature range of 500–1,000°C is ∼3% only for both scum and sludge. The maximum degradation rates are 0.29 mg/min at 360°C for scum and 0.17 mg/min for sludge at 349°C. From Fig. 7(a) and (b), it seems that the incineration of these materials may be carried out within the temperature range of 400–500°C. The ash content in scum and sludge are found as ∼40 and 60%, respectively. From Fig. 7(a) and (b), the calorific value of sludge seems to be lower than scum, which is also supported by the low carbon and high ash in sludge with respect to scum. The significant amount of heat (-8.62 J/mg) released due to the oxidation of scum as shown in Fig. 7(a) indicates that the calorific value of the scum is in the range of municipal solid wastes, and thus it can be used effectively for energy production through incineration.

4. Conclusions

From the above discussion, the following conclusions are made:

(1) Optimum conditions for the removal of color and organic pollutants from pulp and paper industry wastewater are pH: 7, treatment time: 75 min, current density: 115 A/m^2, and interelectrode distance: 1.5 cm.
(2) Under the optimum operating conditions, the percent removals of COD, TOC, and color are found to be 76, 76, and 99%, respectively.
(3) Under the experimental domain, the proposed empirical models can give prediction on COD, TOC, and color removal with error limit of ±7, ±9, and +2 to −6%, respectively.
(4) The scum is more porous than sludge, but both possess similar types of functional groups.
(5) Calorific value of scum is more than sludge
(6) Scum and sludge can be utilized for energy production through incineration followed by aluminum recovery since these contain considerable amount of carbon (in scum ∼38.3% and in sludge ∼23.8%) and aluminum (in scum ∼22.5% and in sludge ∼38.4%).

References

[1] A. Garg, I.M. Mishra, S. Chand, Catalytic wet oxidation of the pretreated synthetic pulp and paper mill effluent under moderate conditions, Chemosphere 66 (2007) 1799–1805.
[2] M. Ali, T.R. Sreekrishnan, Aquatic toxicity from pulp and paper mill effluents: A review, Adv. Environ. Res. 5 (2001) 175–196.
[3] D. Pokhrel, T. Viraraghavan, Treatment of pulp and paper mill wastewater – A review, Sci. Total Environ. 333 (2004) 37–58.
[4] H. Temmink, K. Grolle, Tertiary activated carbon treatment of paper and board industry wastewater, Bioresour. Technol. 96 (2005) 1683–1689.
[5] M. Ghorbani, H. Esfandian, N. Taghipour, R. Kata, Application of polyaniline and polypyrrole composites for paper mill wastewater treatment, Desalination 263 (2010) 279–284.
[6] T.S. Jamil, M.Y. Ghaly, I.E. El-Seesy, E.R. Souaya, R.A. Nasr, A comparative study among different photochemical oxidation processes to enhance the biodegradability of paper mill wastewater, J. Hazard. Mater. 185 (2011) 353–358.
[7] A.M. Amat, A. Arques, F. Lopez, M.A. Miranda, Solar photocatalysis to remove paper mill wastewater pollutants, Sol. Energy 79 (2005) 393–401.
[8] V.C. Srivastava, I.D. Mall, I.M. Mishra, Treatment of pulp and paper mill wastewaters with poly aluminium chloride and bagasse fly ash, Colloids Surf., A 260 (2005) 17–28.
[9] A.L. Ahmad, S.S. Wong, T.T. Teng, A. Zuhairi, Improvement of alum and PACl coagulation by polyacrylamides (PAMs) for the treatment of pulp and paper mill wastewater, Chem. Eng. J. 137 (2008) 510–517.
[10] K.S. Parama Kalyani, N. Balasubramanian, C. Srinivasakannan, Decolorization and COD reduction of paper industrial effluent using electro-coagulation, Chem. Eng. J. 151 (2009) 97–104.
[11] M. Vepsalainen, H. Kivisaari, M. Pulliainen, A. Oikari, M. Sillanpaa, Removal of toxic pollutants from pulp mill effluents by electrocoagulation, Sep. Purif. Technol. 81 (2011) 141–150.
[12] S. Khansorthong, M. Hunsoma, Remediation of wastewater from pulp and paper mill industry by the electrochemical technique, Chem. Eng. J. 151 (2009) 228–234.
[13] E.S.Z.E. Ashtoukhya, N.K. Amina, O. Abdelwahabb, Treatment of paper mill effluents in a batch-stirred electrochemical tank reactor, Chem. Eng. J. 146 (2009) 205–210.
[14] S. Mahesh, B. Prasad, I.D. Mall, I.M. Mishra, Electrochemical degradation of pulp and paper mill wastewater. Part 1.COD and colour removal, Ind. Eng. Chem. Res. 45 (2006) 5766–5774.
[15] L.S. Cleceri, A.E. Greenberg, A.D. Eaton, Standard Methods for the Examination of Water and Wastewater, 20th ed., American Public Health Association, Washington, DC, 1998.
[16] CPPA technical section standard method H5P, Canadian pulp and paper association, Montreal, 1974.
[17] P. Holt, G. Barton, C. Mitchell, Electrocoagulation as a wastewater treatment, Third Annual Australian Environmental Engineering Research Event, 2006.
[18] G. Parker, B. Noller, T. David Waite, Assessment of the use of fast-weathering silicate minerals to buffer AMD in surface water in tropical Australia, 1251–1260. Available from: http://pdf.library.laurentian.ca/medb/conf/Sudbury99/NewTech/NTOP23.PDF (Accessed on 23.01.13).
[19] M. Kobya, O.T. Can, M. Bayramoglu, Treatment of textile wastewaters by electrocoagulation using iron and aluminum electrodes, J. Hazard. Mater. B100 (2003) 163–178.
[20] H.A. Moreno- Casillas, D.L. Cocke, J.A.G. Gomes, P. Morkovsky, J.R. Parga, E. Peterson, Electrocoagulation mechanism for COD removal, Sep. Purif. Technol. 56 (2007) 204–211.
[21] K. Thella, B. Verma, V.C. Srivastava, K.K. Srivastava, Electrocoagulation study for the removal of arsenic and chromium from aqueous solution, J. Environ. Sci. Health A 43(5) (2008) 554–562.
[22] M. Kobya, H. Hiz, E. Senturk, C. Aydiner, E. Demirbas, Treatment of potato chips manufacturing wastewater by electrocoagulation, Desalination 190 (2006) 201–211.
[23] N. Modirshahla, M.A. Behnajady, S. Kooshaiian, Investigation of the effect of different electrode connections on the removal efficiency of tartrazine from aqueous solutions by electrocoagulation, Dyes Pigm. 74(2) (2007) 249–257.

[24] R. Sridhara, V. Sivakumarb, V. Prince Immanuelc, J. Prakash Maranb, Treatment of pulp and paper industry bleaching effluent by electrocoagulant process, J. Hazard. Mater. 186 (2011) 1495–1502.

[25] L. Yao, Z.F. Ye, M.P. Tong, P. Lai, J.R. Ni, Removal of Cr^{3+} from aqueous solution by biosorption with aerobic granules, J. Hazard. Mater. 165 (2008) 250–255.

[26] C.G. Rocha, D.A.M. Zaia, R.V.S. Alfaya, A.A.S. Alfaya, Use of rice straw as biosorbent for removal of Cu (II), Zn (II), Cd (II) and Hg (II) ions in industrial effluents, J. Hazard. Mater. 166 (2009) 383–388.

[27] K.S. Das, A.K. Guha, Biosorption of hexavalent chromium by Termitomyces clypeatus biomass: Kinetics and transmission electron microscopic study, J. Hazard. Mater. 16 (2009) 685–691.

[28] R.T. Arlinghaus, L. Andrews, Fourier transform infrared spectra of alkyl halide-HF hydrogen bonded complexes in solid argon, J. Phys. Chem. 88 (1984) 4032–4036.

[29] M. Huang, L. Chen, D. Chen, S. Zhou, Characteristics and aluminum reuse of textile sludge incineration residues after acidification, J. Environ. Sci. 23(12) (2011) 1999–2004.